1992-02

The density minimum at the Earth's magnetic equator

Olsen, R.C.

Olsen, R.C., The density minimum at the Earth's magnetic equator, Journal of Geophysical Research, 97, 1135-1150,*1992.

JOURNAL OF GEOPHYSICAL RESEARCH, VOL 97, PAGES 1135-1150, FEBRUARY 1, 1992

The Density Minimum at the Earth's Magnetic Equator

R. C. Olsen
Physics Department Naval Postgraduate School, Monterey, California

Observations of the density structure in the plasmapause region reveal the existence of a local minimum in the total electron density at the magnetic equator. Data from the plasma wave instrument and ion mass spectrometer on the Dynamics Explorer (DE) 1 satellite are used to study this phenomenon. The density depletion typically extends from ±5° to ±20° in latitude, and is found at altitudes from 2 to 5 R_E. Density depletions of 10-70% are found, in regions where the off-equator density ranges from 10-1000 cm^{-3}. This density structure is associated with equator crossings where the thermal plasma has been heated over normal plasmasphere values. The heated plasma is the equatorially trapped plasma previously reported from DE 1 and the SCATHA satellite. Within the plasmasphere, the drop in total (electron) density corresponds to a decrease in the cold-ion density, in both H^+ and He^+. There is a rough pressure balance provided by the warm tail of the distribution, which is a few percent by density, but 1-2 orders of magnitude higher in temperature.

1. INTRODUCTION

The structure of the outer plasmasphere and the plasmapause region is the product of the dynamic interactions between processes which empty and fill the magnetic flux tubes from L = 2 to 6 [*Horwitz, et al 1984; Singh and Torr, 1990*]. The nature and evolution of these structures is important to understand because the plasmasphere forms the bulk (by mass density) of the magnetosphere, and because of the dynamic interactions between hot and cold plasmas which determine processes such as the precipitation of ring current particles into the ionosphere.

The difficulty in understanding the plasmasphere structure is the common one in magnetospheric physics: How do we infer global morphology from single satellite measurements? Substantial progress has been made, of course, particularly in terms of the radial structure. The existence of the plasmapause itself was inferred from whistler measurements [*Carpenter and Smith,* 1963], and satellite measurements [*Gringauz et al 1960; Taylor et al* 1965] during the early days of magnetospheric research.

The nature of the plasmapause, understood primarily as a radial structure, evolved rapidly, and reached an interim level of maturity with the emergence of the, OGO-5 mass spectrometer measurements, in conjunction with whistler observations. For example, the dusk bulge was inferred by *Chappell et al* [1970] and *Carpenter* [1970]. Steady state convection models were applied to the plasmapause, as in the work by Chen and Wolf [1972]. Such models produced the concept of a tear-drop shape for the plasmasphere, and provided an interpretation for the dusk bulge. Time dynamic processes such as those involving detached plasma regions were inferred in the work by Chappell [1974]. These processes were modeled and interpreted in terms of time-varying electric field structures which explained many of the observed features [e.g *Chen and Wolf,* 1972].

There was relatively little information .about the latitudinal profile of these plasmapause density structures prior to the launch of Dynamics Explorer (DE) 1 in 1981. The available information was disquieting, however. For example, ISIS 1 measurements in the topside ionosphere (600-3600 km altitude) showed density structures which generally resembled those inferred from whistler measurements and higher altitude spacecraft. Unfortunately, the ISIS measurements showed no indication of the dusk bulge [*Brace and Theis,* 1974]. With the advent of the paired satellites, DE 1 and DE-2, simultaneous high/low altitude measurements became possible. Some success was found in linking the two regions, though evidence of disconnection persisted [*Horwitz et al* 1986].

The behavior of the intermediate latitudes was first addressed by combining DE 1, ISEE 1, and GEOS 2 data [*Decreau et al* 1986]. In this latter work, the plasmapause in the dusk bulge region was often found to demonstrate a uniform density distribution in latitude - e.g. density profiles from DE 1 corrected to account for radial variations (L^{-4}) were essentially flat in the ±40° magnetic latitude range. These measurements were typically consistent with diffusive equilibrium along magnetic field lines. Alternately, at very early stages, the distributions were consistent with collisionless models. In either case, one implication of these observations for plasmasphere filling was that the existing models of plasmasphere filling, which suggested the existence of structures such as shocks, might not be supportable [e.g. *Banks and Holzer,* 1968].

Indications of field-aligned structures were found, however, in other portions of the DE 1 data set [Olsen et al 1987]. Studies of the magnetic equator, at the plasmapause, showed that there was often a heated component to the thermal plasma, which could comprise as much as 50% of the thermal plasma distribution (at densities from 10-200 cm^{-3}). This work was not conclusive on this point, but illustrated two cases where the equatorial region apparently exhibited a local minimum in density, and a local maximum in temperature (see *Olsen et al* [1987],Figures 7 and 10).

This aspect of the DE 1 data set has been explored further, with an emphasis on times where distinct density structures were found that might be associated with latitudinal variations. In this work, it is shown that such structures can be observed, supporting the idea of a Density Minimum field-aligned density/temperature structure which is consistent with some theories of shock-formation in refilling flux tubes [*Singh and Hwang,* 1987]. One necessary caution at this point is that the structures observed here are not necessarily the norm for the plasmapause region, though they appear reasonably common. The struggle to unambiguously identify a latitudinal structure from radial structure precludes a proper statistical study, in the absence of multi-satellite data.

1.1 Satellites And Instrumentation

Data in this article are taken from the Dynamics Explorer 1 (DE 1) satellite. The analysis is based primarily on data from the Plasma Wave Instrument (PWI) and the Retarding Ion Mass Spectrometer (RIMS). Data from the Energetic Ion Composition Spectrometer (EICS) have also been used where appropriate to supplement the RIMS data.

DE 1 was launched into polar orbit on August 3, 1981. The DE 1 orbit is elliptical with an apogee of approximately 23,300 km (4.56 R_E geocentric), an initial perigee of 570 km, and an orbit period of 7 hours. In mid-1982 and late 1983, the orbit was particularly suited to latitudinal profiles in L, with apogee near the equator. The satellite spin axis is perpendicular to the orbit plane, and the spin period is 6 s.

The plasma wave instrument (PWI) provides a spectral analysis of the ambient electric and magnetic field spectrum. These data are used to determine plasma wave density using characteristic plasma wave signatures such as the upper hybrid resonance, or the continuim cutoff at the plasma frequency [e.g. *Kurth et al 1979*]. The portion of the instrument used here covers the 100 Hz to 400 kHz frequency range. This narrow band sweep frequency receiver (SFR) is typically attached to the long electric dipole antenna (215 m tip-to-tip) during the periods of interest. [*Shawhan et al* 1981].

Plasma densities are derived from the PWI data in this paper, primarily from observations of the upper hybrid resonance. These data provide good, unambiguous measurements of total electron density (e.g., *Olsen et al,* [1987]). There are some modest error levels which can occur, even when the data are good (as in the times selected for analysis here).

There are two, related sources of error. The SFR channels are not contiguous, and so if we assume that the peak in the upper hybrid resonance gives the density, that peak can be missed, introducing an error of a few percent in locating the frequency of the peak (the spacing between channels varies from 5-10%). Since the upper hybrid is not a monochromatic signal, there is an error of similar magnitude from the plasma waves natural amplitude distribution. Since the density goes as the square of the plasma frequency, these problems produce a 10-20% error in any one density determination.

RIMS provides the energy, angle, and mass analysis of the core, or thermal plasma. It consists of a retarding potential analyzer (RPA) followed by an ion mass spectrometer (IMS). The RPA is swept in voltage from 0 to 50 V, providing energy analysis, while the IMS scans from 1 amu to above 32 amu (energy dependent). Two parallel mass channels are available in each of three detector assemblies, measuring ion species with mass ratios of 1:4. For the work reported here, the mass spectrometer settings used were those that selected H^+/He^+ or He^+/O^+.

The high energy limit of the RIMS passbands is determined by the mass spectrometer. For H^+, the upper limit is several hundred eV; for He^+ the limit is above 50 eV; and for O^+ slightly below 50 eV. One detector assembly views perpendicular to the spin axis, with the others viewing parallel and anti-parallel to the spin axis. Pitch angle distributions of the core plasma can be obtained from the radial viewing detector, with an angular resolution of about 20° in the spin plane. The angular width is approximately 110° in the complementary direction. The RPA grids on the radial detector became shorted late in 1981, preventing useful RPA analysis for most of the data considered here. The end heads (also termed the ±Z heads), view along the spin axis, with 110° acceptance windows oriented perpendicular to the magnetic field. The RPA data from these latter detectors remains valid [*Chappell et al* 1981].

Analysis of the core plasma with the RIMS instrument results in temperatures which are good to ~30%, for the data sets considered here. Absolute densities can be difficult to obtain with RIMS, after the RPA failure, but relative H^+ to He^+ values can be determined to within a few percent by intercalibrating the HI/LO mass channels and taking the ratio of the fluxes, so long as the plasma is reasonably isotropic and not strongly affected by satellite charging effects.

The RIMS data can be supplemented by observations from the EICS instrument. EICS provides energy, mass, and angular analysis of the ion distributions up to 17 keV in broad energy intervals. The EICS design consists of an RPA, followed by an electrostatic analyzer (ESA), followed by mass analysis. For the periods analyzed below, 15 energy bands were used to cover the full energy range. The low energy limit of the lowest energy band is set by the RPA. It could be set to voltages from zero up to ~85V. It was set to 10V during the periods considered here. (That is, ions with energies more than 10 eV above the satellite potential are accepted.) The high energy limit of the low energy channel is set by the ESA at about ~125 eV. The second energy channel was centered at 230 eV, with a full width at half maximum (FWHM) of ~160 eV. The third channel was centered at 430 eV, with a FWHM of ~175 eV. EICS has a radial field of view, like the RIMS radial detector. The angular resolution is 15° by 10° at the highest energies, but is somewhat broader in the lowest energy channels [*Shelley et al* 1981].

2 OBSERVATIONS

The program of study developed to address the latitude structure of the plasmapause region began with a project using complementary ISEE 1 and DE 1 density profiles. The idea was to use the dual spacecraft measurements to reduce the ambiguity in the DE 1 latitude profiles. Due to the ultimately limited overlap in data sets, this was only moderately successful. The one major exception was the first case studied, which was shown by *Olsen et al* [1987]. This survey was useful, however, because. it supported the commonly held L^{-4} dependence for plasma density which is typically used to describe the plasmasphere [Chappell et al, 1970]. This led to the plotting of the normalized density in all routine analysis. Densities are normalized by multiplying by L^{-4}. This made it much easier to sort out the radial dependence in DE 1 data sets. Work by Gallagher et al [1988] suggests that the L^{-4} dependence used here is too simplistic. This should not strongly affect the results, however, since the analysis is not sensitive to the assumed rate of density decrease, for the effects inferred here.

Five examples are shown, ranging in local time from 0300 LT, through local midnight, and around through dusk to local noon (1100). Unfortunately, DE 1 does not sample the dawn sector at high altitude/low latitude. The examples are. ordered in terms of increasing plasma density, and decreasing altitude. The first two are in the outer region of the plasmapause, in what would typically be considered refilling regions. The remaining examples are within the plasmasphere, in regions where cold, isotropic plasma dominates the measurements.

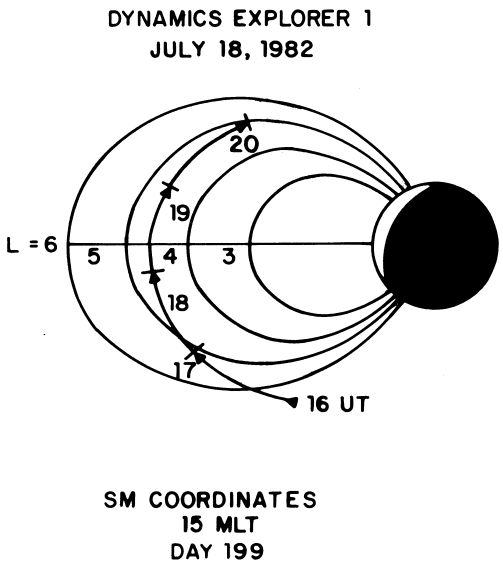

Figure 1. DE 1 orbit for 18 July 1982 (day 199), in SM coordinates.

2.1 Plasmapause, 1500 MLT

The first two examples come in the afternoon/dusk region of the outer plasmasphere, with the DE 1 apogee coming near the magnetic equator. The first of these, on July 18, 1982 (day 199) provides measurements made in regions of relatively low plasma density (10-20 cm^{-3}). The orbit for DE 1 is shown in Figure 1, in SM coordinates. The orbit has been rotated into a common local time. DE 1 is in the mid-afternoon sector, and stays near L = 4.5 for a substantial portion of the equator passage.

The total electron density profiles derived from the plasma wave data are shown in Figure 2. The electron density (lower panel) shows a nearly monotonic variation, with faint indications of a local decrease in density at -20°, and a subsequent rise at ~+15° magnetic latitude. The data are normalized by a factor of L^4 and replotted in the top panel. Once the data are normalized, it is clear that the region from -20 to +20 degrees magnetic latitude is a region of reduced density. There may be a modest local maximum in the density profile within 5° of the equator, but the variation is close to the one channel resolution of the instrument.

RIMS data are shown in Plate 1 in the spectrogram format typically used for these data. [e.g., *Olsen et al* 1987]. The top two panels show the H^+ data, the bottom two panels show the He^+ data. In each pair of spectrograms, the upper panels shows the retarding potential analyzer (RPA) data from the end head, which views parallel to the spin axis. Since the satellite spin axis is perpendicular to the magnetic field, the detector nominally views the isotropic plasma, and ions moving perpendicular to the magnetic field. The lower panel in each pair shows the data from the detector viewing radially away from the satellite, perpendicular to the spin axis. These are integral fluxes, taken at zero volts on the RPA. The data are ordered by spin phase, with measurements taken looking in the ram direction defining zero spin phase. (The detector is viewing parallel to the satellite velocity vector at 0° spin phase.) Dotted white lines indicate the spin phase directions corresponding to ion measurements at 0° and 180° pitch angle.

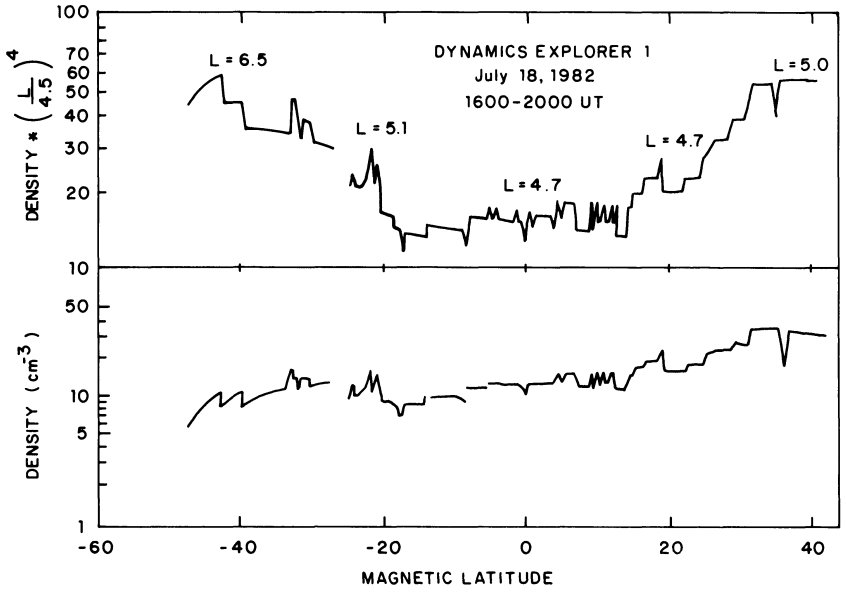

Figure 2. DE 1 electron density profiles for 18 July 1982 (Day 199). The top the normalized profile versus latitude, the bottom panel shows the total electron density.

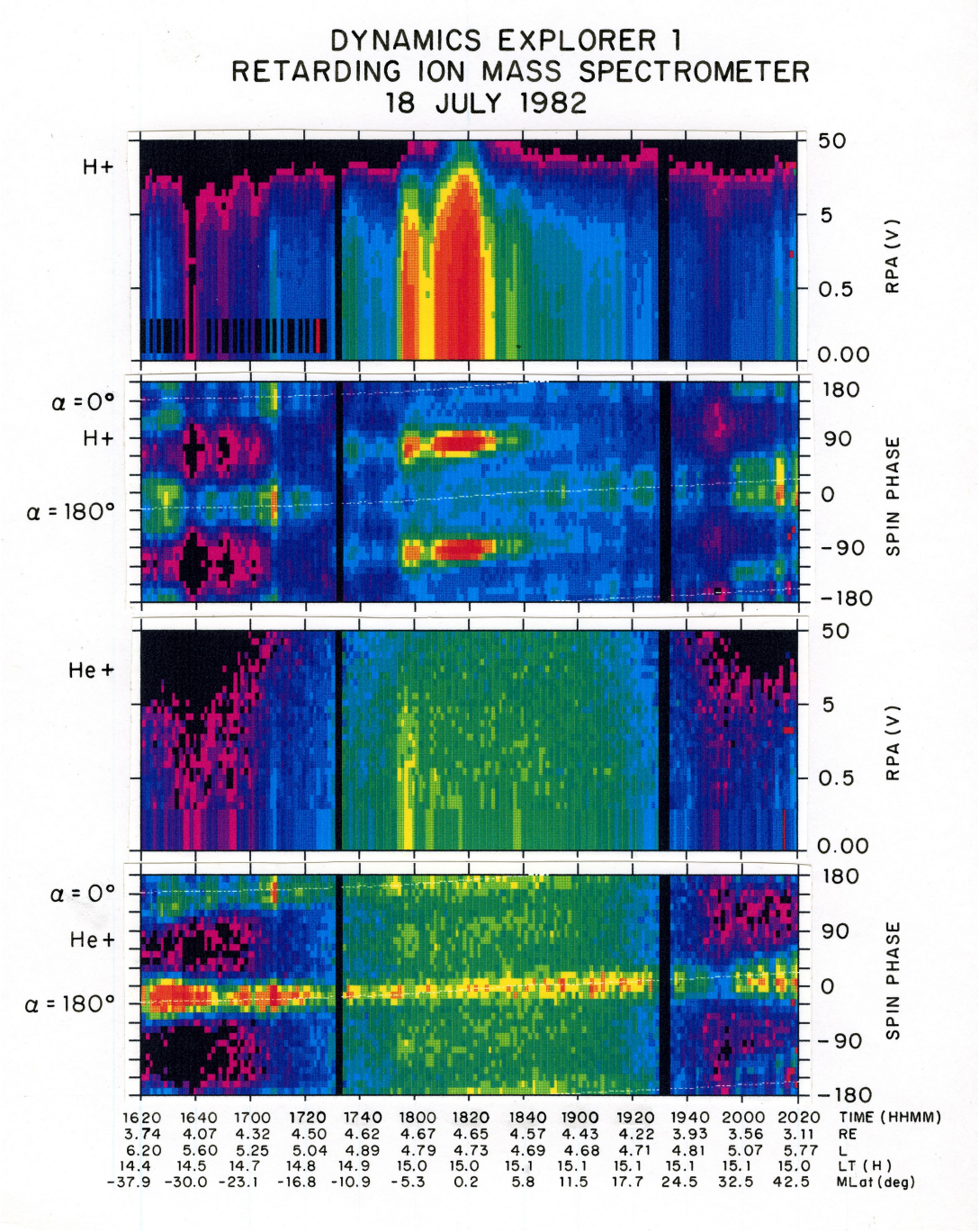

Plate 1. DE 1 data from 18 July 1982. H^+ and He^+ data from RIMS are shown. Particle count rate (flux) is color coded, with low/zero counts plotted as purple, then blue; high counts as orange and red. The top two panels show H^+ data, the bottom two, He^+ data. The color scales were varied to make the salient features visible. The H^+ RPA data are scaled from log counts = 0.8 to 2.4 (e.g. 6-250 counts/accumulation). The He^+ RPA data have been multiplied by 50 to bring them onto the H^+ count rate scale. The He^+ scale is thus effectively 0.1 to 5 counts/accumulation). The H^+ spin phase data are scaled from 1 to 40 counts/accumulation, the He^+ spin phase data from 2 to 63. These peculiar scales are partially made necessary by channeltron degradation (particularly in the radial H^+ detector), but primarily by the curious dynamic range of the data set.

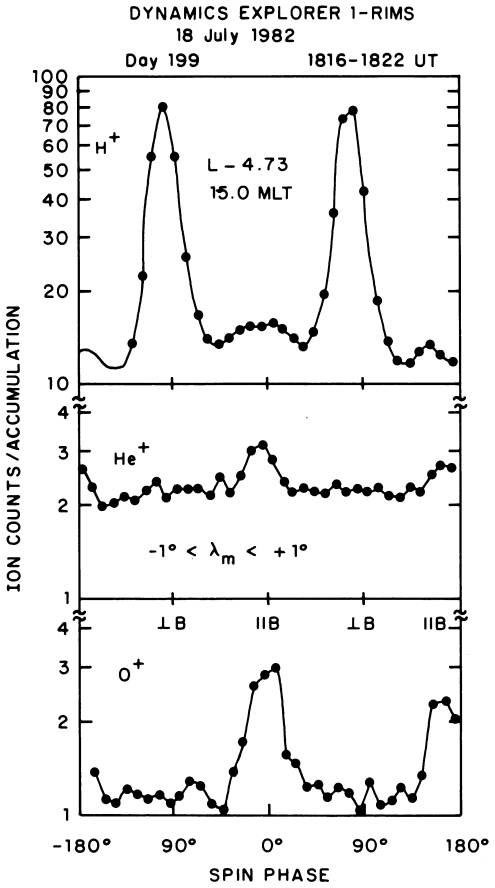

Figure 3. Pitch angle distributions for H^+, He^+, and O^+ on 18 July 1982 (Day 199). The peak H^+ flux is ~3 × 10^6 ions/cm^2 s ster. The peak He^+/O^+ fluxes are 3 × 10^4 ions/cm^2 s sr.

In both H^+ and He^+, the spin phase plots indicate that the plasma away from the equator is field-aligned. These field-aligned ion distributions are characteristic of the region outside the plasmasphere, and are nominally low-energy ion flows from the ionosphere into the magnetosphere. Within 20° of the equator there is a warm isotropic background distribution in H^+ and He^+. Within 5°-7° of the equator, the field-aligned H^+ distribution is superseded by a sharply peaked, equatorially trapped distribution (1750-1840 UT). The end head data (90° pitch angle) energy analysis shows increased energy and flux, particularly in the +6° latitude range.

Figure 3 illustrates the pitch angle distribution at the equator in line plot format. This six-minute average makes clear the order of magnitude anisotropy in the H^+ distribution. It is clear that He^+ is primarily field-aligned, as is the O^+. The relative efficiency of the He^+/O^+ sensor is a factor of four higher than that of the H^+ sensor at this time; the H^+ flux is ~100 times the minor ion flux.

Magnetic activity was high in the interval preceding these measurements, with a large magnetic storm beginning on day 194. *Dst* reached -325 gamma at the beginning of day 195. The ring current had largely recovered by the time of these measurements, but *Kp* was still moderately high, at levels of 4-

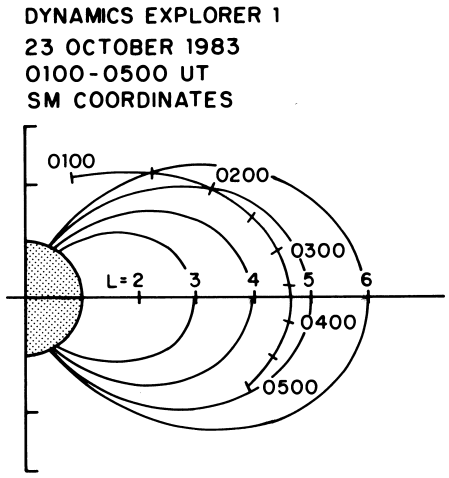

Figure 4. DE 1 orbit plot for 23 October 1983 (Day 296) 0100-0500 UT.

and 3+ during this time period. Similar levels held while these particles were drifting through the midnight to dawn region.

This example illustrates the sort of broad, slowly varying profile often found outside the plasmasphere. Associated with the density minimum is a transition from field-aligned to trapped distributions. *Olsen et al* [1987]

(Plate 3) show a similar case for H^+ distributions. The trapped and field-aligned distributions are not of necessity exclusive, however. Regions of overlap are clearly found, as well [e.g. *Decreau et al* 1986, Plate 1]. The next example is also in this latter category, with field-aligned and trapped distributions co-existing at the equator.

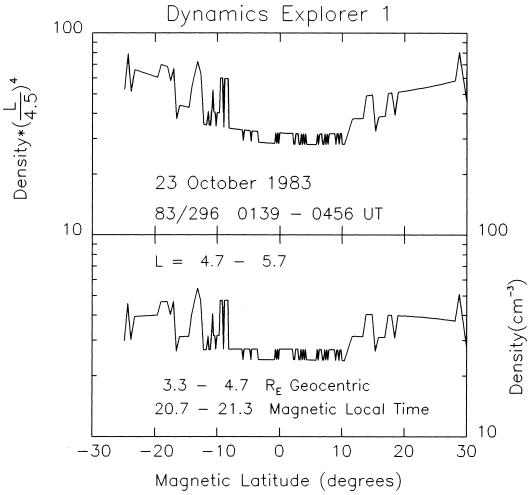

Figure 5. DE 1 data from 23 October 1983 (day 296). The top panel shows the normalized electron density profile versus magnetic latitude. The bottom panel shows total electron density versus magnetic latitude.

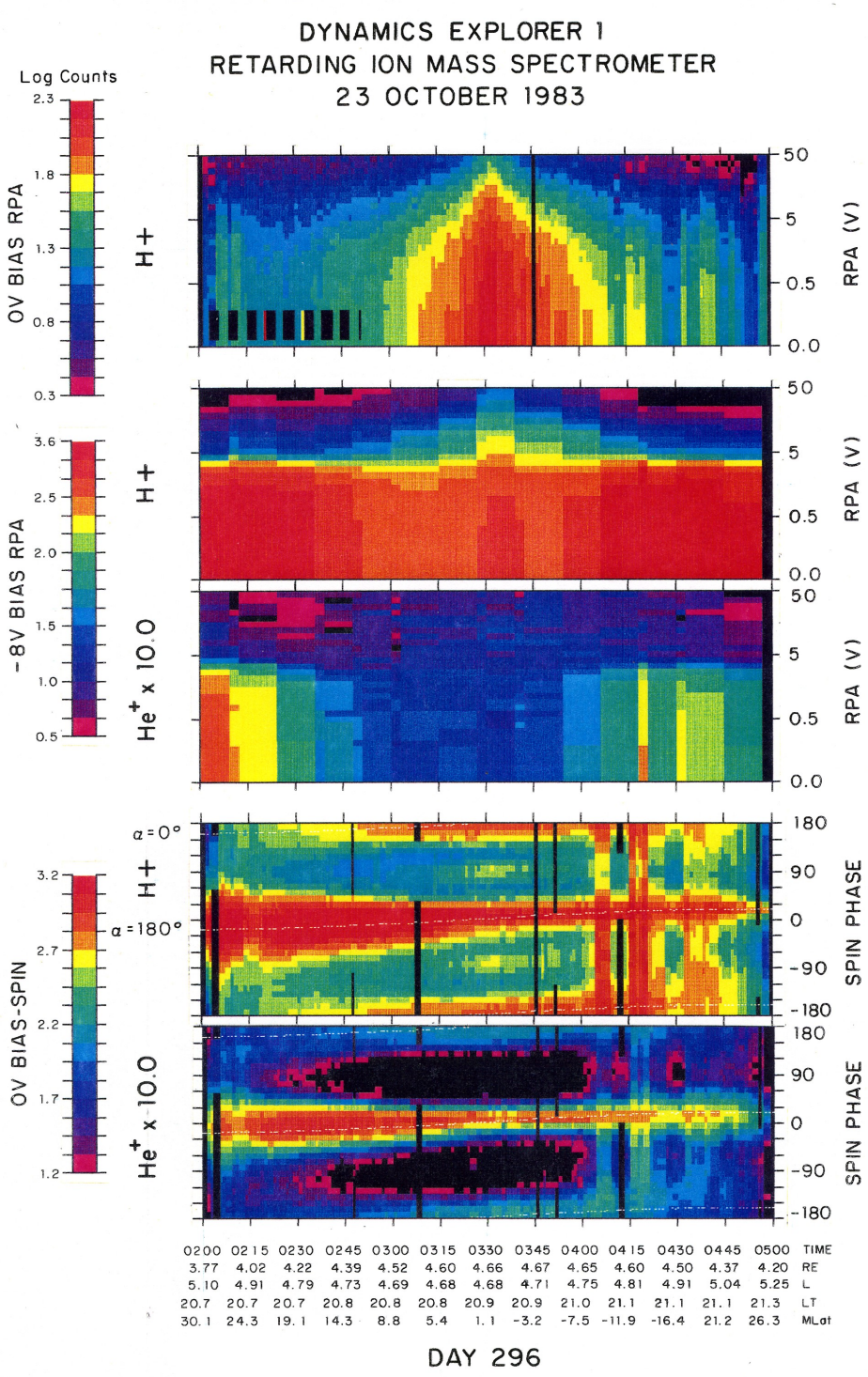

Plate 2. DE 1 data from 23 October 1983 (day 296). The top panel shows H^+ data taken for 0V bias on the aperture plate. The second panel shows H^+ data taken at -8V bias. The third panel shows He^+ data taken at -8V bias. The fourth and fifth panels are spin-phase plots, from H^+ and He^+ respectively. The He^+ data plotted in the bottom panel have been scaled up by a factor of 10. The 0V bias and -8V bias RPA data were plotted with different count rate scales, and have their own color bars, as do the two spin phase plots. The 0V bias RPA data range from 2-200 counts, the -8V bias RPA data from 3-800 counts. The spin-phase plot for H^+ is scaled from 16 to 1600 counts/accumulation.

2.2 Plasmapause, 21 MLT

The second example is again in the dusk region, outside the plasmasphere. This example provides data taken by RIMS during a period of aperture bias cycling on 23 Oct 1983 (day 296). These data are useful because RIMS is able to view the core, low energy plasma away from the equator at density levels from 10-100 cm^{-3} [*Olsen et al* 1986]. Figure 4 shows the DE orbit for the time period of interest. The satellite is grazing the magnetic field line at the plasmapause, at local dusk.

Figure 5 shows the density profile for this time period. The bottom panel shows that there is a local minimum in the total electron density at the equator, even though the satellite is at minimum L at this point. The minimum occurs in the L = 4.2-4.7 range, with a decrease from 50 down to 30 cm^{-3}. The normalized density distribution (top panel) suggests that there is a broader decline over the latitude range observed here, as well as the factor of 2 decrease obvious in the bottom panel. This broad profile is indicative of the early, collisionless, conditions expected in a refilling region [*Decreau et al,* 1986, Figure 7]

The RIMS data are shown in Plate 2. The top panel shows H^+ RPA analysis for +Z (end head) data taken at 0 V aperture bias. Warm isotropic/trapped plasma is visible in this detector from 0200-0500, as is typically found outside the plasmasphere proper. (There is no measurable flux of He^+ at 0V aperture bias.) The spin phase plots, shown in the bottom two panels, indicate that the observed portion of the low energy 0plasma distribution is primarily field-aligned (bi-directional) for most of this period, in both H^+ and He^+. EICS does not observe this field-aligned distribution, indicating that the energy of the field-aligned H^+ ions is less than 10 eV (above the spacecraft potential - a few volts positive in this density regime).

Intensification of the H^+ flux in the end head (the yellow-red region) from 0300-0400 indicates enhanced temperatures at equator. RIMS H^+ data from the radial detector, and EICS data, show that this enhanced flux is of equatorially trapped ions, with energies which reach -100 eV. (This is shown by the two yellow regions near the middle of the fourth panel.) By contrast, there is not an equatorially trapped He^+ distribution (bottom panel).

Plate 2b shows H^+ data taken from +Z detector using an aperture bias of -8V. The aperture bias brings the low energy core plasma into view, in spite of the positive satellite potential. (These are the red/orange regions from 0200-0230 and 0400-0500). The third panel shows He^+ data taken with -8V bias. There is a cold He^+ background distribution, visible away from the equator. Near the equator, the He^+ fades from view. The fading from view of the cold He^+, and the decrease in the H^+ flux, can have two (related) interpretations. If the relative depletion in plasma density is associated with a drop in the He^+ density, the cold plasma will fade from view as the density drops, and be superseded by the heated plasma. This is consistent with these measurements, and many others made with and without aperture bias cycling. Of course, as the total electron density drops from ~40 to ~25 cm^{-3}, the satellite potential becomes more positive, thus further excluding cold plasma from view. In this latter view, the disappearance from view of the cold He^+ may not indicate the total exclusion of cold He^+ from the equatorial region.

The magnetic activity level associated with these measurements was lower than in the previous example. The last previous storm began on day 290, and *Dst* reached -67 gamma. The magnetosphere had recovered from this minor storm by day 296. *Kp* had reached 5 at the beginning of day 295, then declined more or less steadily to the level of 2+ at the beginning of day 296.

This example is typical of the observation set obtained in late 1983, with aperture bias sequencing, in the outer plasmasphere, in the dusk bulge. There is a modest decrease in plasma density, and heating of the H^+. The cold, isotropic He^+ disappears, but is not replaced by a heated distribution.

2.3 Inner Plasmasphere, 3MLT

The third example comes from January 8, 1982. This is again an example with equatorially trapped plasma distributions, but within the plasmasphere, at L = 3.5. The subsequent example will show data from a similar region, at a time when the equatorial plasma is ~isotropic. The orbit is illustrated in Figure 6. The SM coordinates of the DE 1 orbit are rotated into the 0300 local time plane. The satellite passes out through the outer plasmasphere as it crosses the equator, passing through a region of heated plasma. This region is indicated by the cross-hatched area in Figure 6. The top panel of Figure 7a shows the electron density plotted versus "L". There is a decrease in density centered at L = 3.5 of almost one order of magnitude. This is further indicated by overplotting an L^{-4} density profile. The density is replotted versus magnetic latitude in the bottom panel of Figure 7b. It can be seen that the density decrease is associated with the equator crossing. The upper hybrid resonance cannot be measured prior to 1945 UT, since the electron gyrofrequency exceeds the plasma frequency. This means that the high latitude plasmapause cannot be tracked with the PWI data. Further information can be obtained from RIMS, however.

Plate 3 is a color spectrogram for the data from RIMS. The heating region noted above in the orbit plot (Figure 6), corresponds to the large red area in the top panel, which is the RPA analysis for H^+ measured along the spin axis (nominally 90 degree pitch angle). Higher fluxes, and higher retarding voltages, are indicative of warm, heated plasma. The next panel shows H^+ data from the radial detector, providing the angular distribution for the integral proton flux. From 1930-2018 UT, the angular distribution is peaked along 0° spin phase. This is characteristic of an isotropic, 'rammed' distribution, where the satellite velocity is larger than, or comparable to the random thermal velocity of the core plasma. There is a transition from isotropic, rammed plasma, to a pancake distribution (peaked at 90/270 degrees) at 2018 UT. The distribution becomes isotropic, again, at 2027 UT, and then field-aligned (peaked at 0/180 degrees) from 2049-2100 UT. This last transition at 2049 UT is associated with the plasmapause. There is also a plasmapause transitition at 1930 UT, with poorly defined pitch angle distributions.

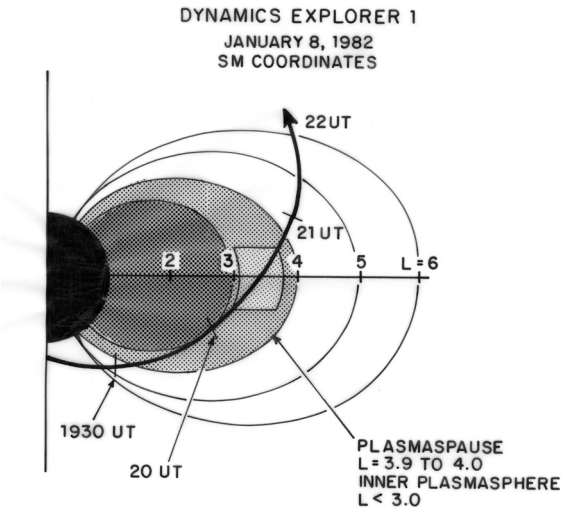

Figure 6. Orbit plot for 8 January 1982 (day 8). The satellite orbit is indicated as solid line. The inner plasmasphere (L<3) is shaded. The equatorial interaction region (heating, equatorial noise, density minimum) is indicated with cross-hatched region from L = 3 to 4. The orbit has been rotated into a common local time (0300).

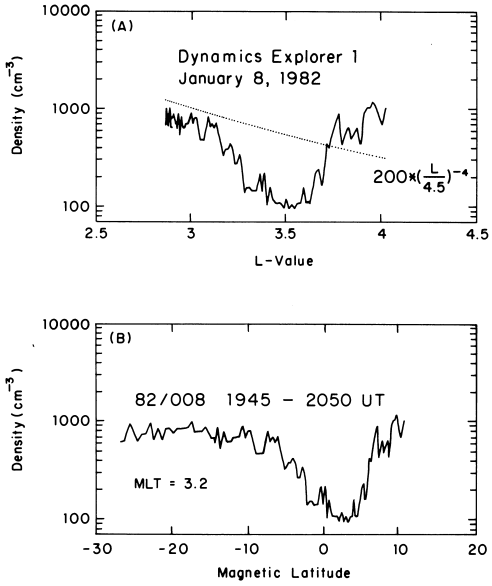

Figure 7. Electron density profiles for 8 January 1982 (Day 8). (a) Density versus McIlwain "L" value. (b) Density versus magnetic latitude.

The two plasmapause crossings both occur at L a 4.0. The high latitude crossing is at -47° magnetic latitude. This coincides nicely with the plasmapause at L = 4.0 observed at 2050 UT, at 10° magnetic latitude. As the orbit plot (Figure 6) shows, this helps eliminate radial variations as the cause of the density variations observed on this day.

The He^+ data are shown in the bottom two panels. The He^+ behaves more-or-less in the same manner as H^+. The main difference is the apparent localization of the most intense flux at the boundaries of the density minimum, at ~2020 UT and ~2035 UT. (A similar localization of the He^+ heating will be shown in the final example, from 14 March 1983.)

The spin curves are shown for data taken at L = 3.4 in Figure 8. This is the L shell at which DE crosses the magnetic equator, at 2024 UT. As shown in the orbit plot, the same region is crossed at 40° magnetic latitude at 1934 UT. The plasma at high latitude (2.0 R_E geocentric), is mostly isotropic, though there are asymmetries in the H^+ and O^+ data. Though not large, the asymmetries make it difficult to fit the H^+ spin curve and obtain a definite value for the density. The H^+ density is 300-500 cm^{-3}, the He^+ density is 50-60 cm^{-3}, the O^+ density is ~1 cm^{-3}. Ion temperatures vary from 0.6-0.7 eV for the light ions, to 1.0 eV for the O^+.

The anisotropic distributions at the magnetic equator can't be fitted for density; but the total electron density is ~140 cm^{-3}. This is a factor of 2-3 below the total density observed at high latitude.

One peculiarity of this pass is that it provides one of the rare measurements of equatorially trapped O^+. The O^+ ions are only briefly heated, with the primary trapped flux observed from 2020-2025 UT, at the first density boundary. This can be seen in the bottom right panel, in the peak between 90° and 180° spin phase. {There presumably would be a peak perpendicular to *B* near 0° spin phase, but it is obscured by the rammed, isotropic, background plasma.)

Data from the Energetic Ion Composition Spectrometer (EICS) (not shown here) show significant H^+ fluxes in the second energy channel, centered at 230 eV, but not in the third energy channel. This observation shows that the H^+ distribution does not extend above 340 eV. In addition, the O^+ fluxes visible in the RIMS data are found in the lowest energy EICS channel. EICS also shows the trapped He^+ distributions, with characteristics similar to the H^+, in the lowest energy channel.

Magnetic activity is low for this example, with negligible storm activity (*Dst*) in the prior ten days, and *Kp* at 3 or less. As in the previous examples, the density minimum is associated with heated plasma distributions. In this case, it is clear that most of the heating is in the perpendicular direction. This makes it difficult to calculate the pressure variation across the density boundaries, since the parallel temperature cannot be easily extracted from the radial detector data. This limitation is avoided in the final two examples.

2.4 Inner Plasmasphere, Local Midnight

The last two examples show primarily isotropic plasma, but at elevated temperatures, at the equator. The first of these shows a relatively minor decrease in density, over a relatively narrow latitude range. The measured portion of the ion distribution remains isotropic, and this allows reasonably good measurements of density and temperature.

Figure 9 shows the orbit on March 15, 1982 (Day 74). The satellite was outbound, rising up to the equator from the southern hemisphere while skimming the L = 3 field line, crossing the equator at L = 3.4, finally crossing the plasmapause at L = 4.5 at 16 degrees magnetic latitude.

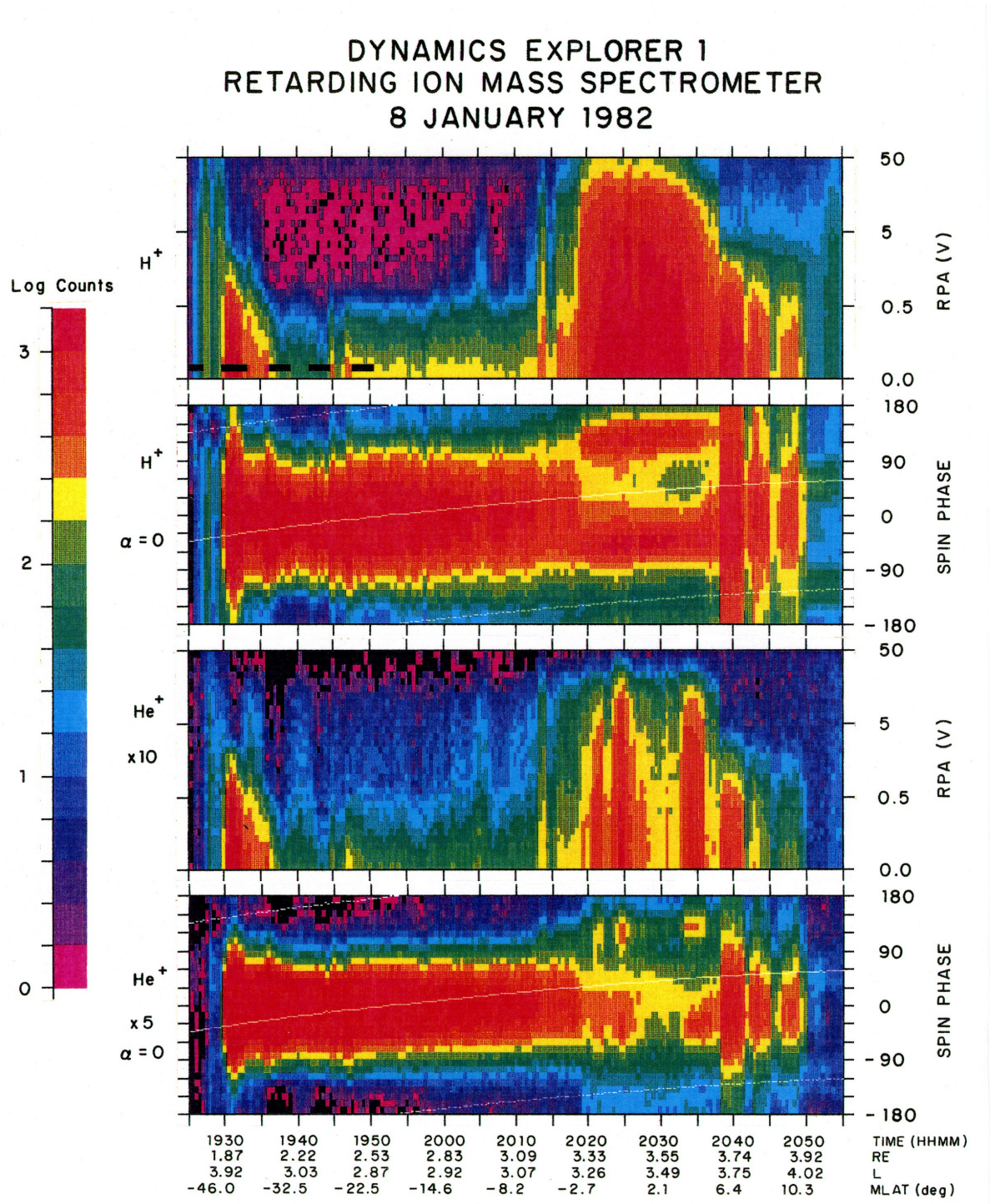

Plate 3. DE 1 data from 8 January 1982. The top panel shows H^+ RPA analysis (Z detector), the second panel the spin phase analysis (R detector). The bottom two panels show the He^+ data. The He^+ RPA data have been scaled up by a factor of 10, the He^+ spin phase data have been scaled by a factor of 5. The magnetic equator is crossed at 2025 UT, at 3.45 Re, 3.2 MLT.

The density profile versus L is shown in Figure 10*a*. The dip at L = 3.4 coincides with the equator crossing. The plasmapause occurs at L = 4.5. The density profile is replotted versus magnetic latitude in Figure 10*b*. There is a gradual decline, mirroring the increase in L, with a factor of 2 decrease at the equator. One curious aspect of the radial density profile is that an L^{-4} dependence describes the data in the southern hemisphere, but not in the northern hemisphere.

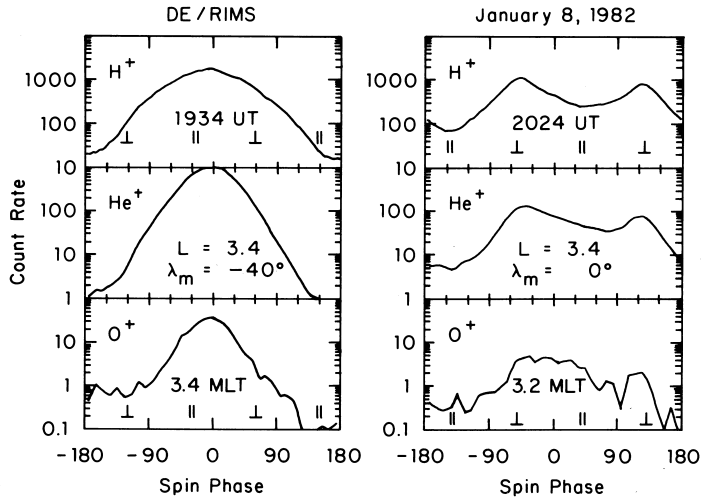

Figure 8. RIMS data taken at L = 3.4, at 1934 UT and 2024 UT, Day 8. The satellite is at 2.0 and 3.4 R_E, geocentric distance, respectively. The perpendicular and parallel symbols indicate the spin phase for 90°/270° and 0°/180° pitch angles.

The thermal plasma data are shown in Plate 4. In this plate, the H^+ and He^+ energy analysis, and the He^+ angular distributions are shown. The H^+ angular distributions are not available for this time, due to channeltron degradation induced by the aperture bias mode [*Olsen et al,* 1986]. The bottom panel shows the spin-phase angular distribution for the He^+ ions measured at 0V retarding potential. Data are selected from the subset of times when there is no bias on the aperture plate. The plasma is seen to be isotropic throughout this time segment, with the exception of the last 5-10 minutes. From 0450-0500, the angular distribution is a bi-directional, field-aligned distribution, as is typically found outside the plasmasphere.

Plates 4a and 4b show the RPA analysis from the +Z detector, which views parallel to the spin axis, nominally at 90° pitch angle ions. Cold (isotropic) H^+ and He^+ ions are measured on either side of the equator. At the equator there is a decrease in ion flux for RPA voltages below 2V, indicating a drop in the cold plasma density. A warm population of H^+ appears briefly as indicated by the increase in flux above the 2V retarding potential level, at 0411 UT. There is also a brief increase in the EICS measurements of 0.01 - 1 keV H^+, in the isotropic/perpendicular direction (data not shown). Cold plasma is still present, but at reduced levels, in both H^+ and He^+.

Analysis of the thermal plasma data shows that prior to the equator crossing, 93% (±3%) of the plasma is H^+; He^+ makes up most of the remainder (ignoring O^+ and other trace constituents). The H^+ and He^+ have a common temperature of ~0.45 eV. At the equator, the core H^+ and He^+ densities drops by a factor of 2 or 3, and the core plasma temperature increases slightly to ~0.55 eV. There is a warm tail which appears briefly in the H^+ data at 0411 UT. The tail can be characterized with a density of 0.35 cm^{-3}, and a temperature of 35 eV. By density, this is less than 1% of the total H^+ population. If there was heated He^+, at 1% or less of the total He^+ density, it would be invisible at these flux levels.

Magnetic activity is low at this time. The previous 'major' storm came at the end of day 60, reaching a *Dst* of -211 gamma. *Kp* was steady at 3 or less at this time.

2.5 Inner Plasmasphere, 11 MLT

The final example shows a density minimum at the lowest radial distance found so far, from 2.0-2.3 R_E. Figure 11 shows the orbit segment for 14 March 1983 (Day 73). The satellite is rising from perigee, as it crosses the magnetic equator at 2.1 R_E. The satellite reaches the plasmapause at ~1512 UT, at L = 3.5. Figure 12 shows the density profile versus L in the top panel, and the density profile versus latitude in the bottom panel. The decrease in density at the equator, at L = 2.5, is almost an order of magnitude.

The major decrease in plasma density begins at L = 2, +8° magnetic latitude, at 1441 UT; the subsequent increase occurs at 1500 UT, -14° magnetic latitude, L a 2.7. The plasmapause is encountered at -23° magnetic latitude, L - 3.5. The RIMS and PWI data show flat density profiles at high latitudes, until a drop in flux is encountered at 1.34 R_E, at 1424 UT. This plasma boundary, at L =~2.5, appears to be an altitude effect, rather than the plasmapause, but this is not a major point.

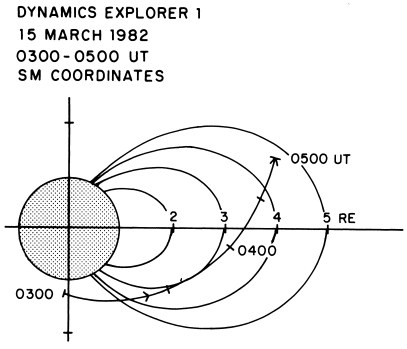

Figure 9. DE 1 orbit for 15 March 1982 (day 74)

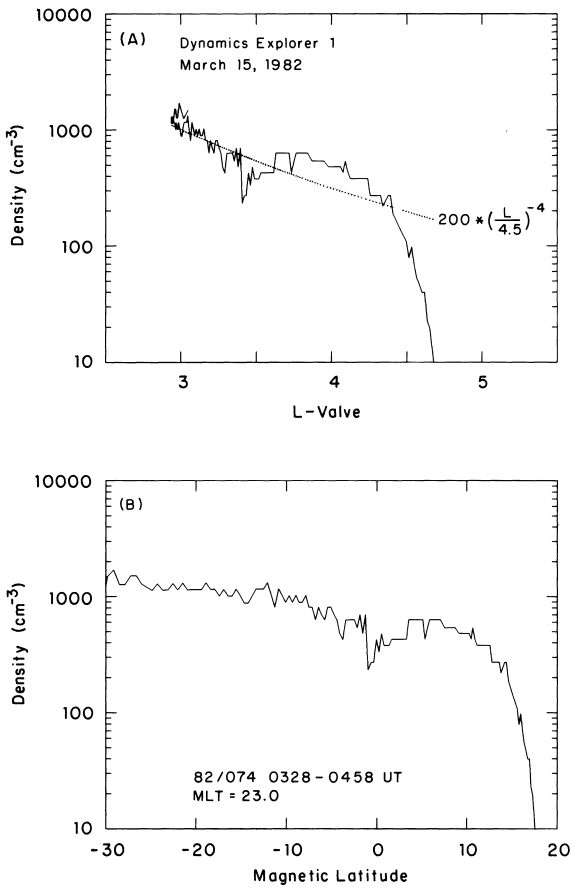

Figure 10. DE 1 electron density profiles for March 15, 1982 (day 74). (a) Electron density versus L. An L^{-4} profile is superimposed. (b) Density versus magnetic latitude.

The main thing is that there is no decrease in flux associated with crossing the L=2 field line (at 1430 UT) which maps to the density minimum. This event is fairly unique in having the proper orbit, and telemetry coverage, to achieve this multi-point measurement along the field line.

The magnetic activity associated with this set of observations is substantially higher than in the other examples. There was a reasonably large magnetic storm preceeding this orbit, which peaked at a *Dst* of -132 gamma at the end of day 71, and *Kp* was 4+ at the time of these measurements. *Kp* increased sharply from 2 to 5- and 5+ during the 12 hour period when these particles rotated through the post-midnight sector. This increased level of activity may explain the unusually low altitude for the density minimum, and the peculiar nature of the ion data which are shown next.

The nature of the thermal plasma measurements is shown in Plate 5 Spin phase and RPA-time plots are shown for the H^+ and He^+. The H^+ and He^+ RPA data show a surprisingly different character. The H^+ angular distribution is largely isotropic throughout this period. (There is a saturation effect in the H^+ data from 1420-1445 UT, producing the curious asymmetry in spin phase.) Field-aligned distributions appear at the plasmapause, encountered at 1513 UT. At the equator the proton temperature increases as seen in the RPA data from 1445-1500 UT (top panel). A trapped distribution appears briefly above the 'rammed' isotropic distribution in the spin-phase plot. This trapped population is most evident from 1445-1450 UT in the spin phase plot at +120° spin phase. EICS survey data (not shown) indicate that the equatorially trapped H^+ ions extend up to the second (230 eV) channel, but the largest flux is in the lowest energy channel.

(Note that sensitivity of the RIMS low mass channel (H^+) has decreased substantially at this time, due to channeltron decay. The RIMS high mass channel (He^+) has an efficiency which is 7-10 times higher than that of the low mass channel, in the radial detector. The H^+ and He^+ detectors used for the RPA data from the end heads are roughly equal in sensitivity.)

The He^+ ion flux (density) decreases at the equator by a factor of 2. The He^+ is not noticeably heated at the equator. There is, however, a warm He^+ distribution at either side of the equator, bracketing the region with the density minimum. These heated He^+ ions may be associated with wave power observed in the PWI data at 5-10 Hz, which is an appropriate frequency range for ion cyclotron waves associated with He^+ or O^+. (*B* varies from 3000 nT down to 2000 nT during this period).

The O^+ ions (not shown) form a cold, isotropic distribution which decreases ~monotonically in ion flux (density) with altitude. The O^+ distribution shows no obvious effects at the equator crossing, though the temperature increases slightly after 1450 UT.

Detailed analysis of the RPA and spin phase data shows that H^+ is the dominant ion throughout this period, at ~90% of the total ion density. Away from the equator, the H^+ density is ~1800 cm^{-3}, with a temperature of 0.4 eV. The cold He^+ density is ~100 cm^{-3}, also with a temperature of 0.4 eV at 1435 UT. The O^+ density is rapidly dropping through this period. At 1435 UT, the O^+ density is ~3 cm^{-3}, with a temperature of 0.25 - 0.4 eV.

At the equator, the O^+ shows no major change, but gradually increases in temperature to 0.5 - 1.0 eV, as the density drops below 1 cm^{-3}. The core He^+ density drops by a factor of 5-6, down to a value of ~15 cm^{-3} at the equator, and the temperature rises slightly, to 0.5 eV. A hot 'tail' forms, which is somewhat anisotropic, with a temperature of ~15 eV, and a density of 0.6-0.8 cm^{-3}. The H^+ core plasma is difficult to characterize, because of the lack of good spin phase data. In particular, it is not possible to say if the H^+ is isotropic, or to establish the degree of anisotropy. The RPA data are consistent with H^+ densities of a few hundred per cm^3 (the bulk of the plasma), at a temperature of ~0.5 eV. The warm tail is characterized by a temperature of 25 eV, and a density of 10-20 cm^{-3}.

These data, though not typical in L-shell (altitude), do illustrate a recurring aspect of the DE 1 data in the plasmasphere. In the region of the density minimum, there is a modest increase in the core plasma temperature. A warm tail forms above the core distribution. The He^+ ions are either not substantially heated, or are heated in proportion to the density ratios for the cold plasma.

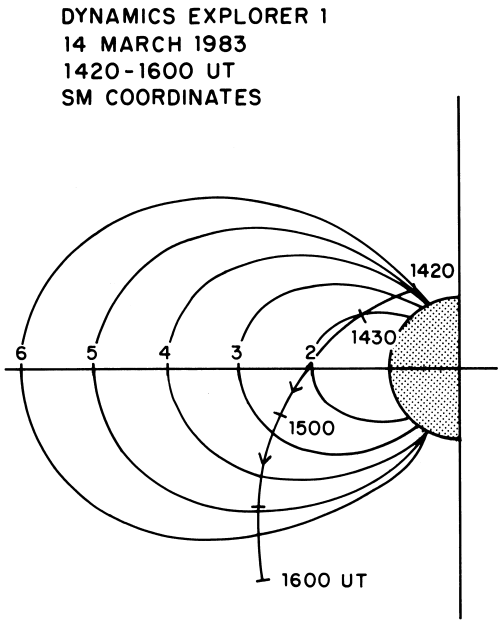

Figure 11. DE 1 orbit plot for 14 March 1983 (Day 73).

2.6 Summary Of Observations

The observations presented here were selected to provide a demonstration of the minimum in plasma density observed along magnetic field lines at the equator, at a variety of density levels. A cross-section of local-times/altitudes was chosen, with the satellite orbit restricting the possible combinations. The cases shown here are among the clearer cases for each region, with deep sustained minima. The primary selection criteria was an attempt to avoid times where there was obviously a radial density structure which overwhelmed the latitudinal profile. One simple criteria which eliminated many good candidate examples was a requirement that both sides of the equator be sampled, that is, that both density boundaries be observed. It is the concern with possible radial density structures which makes it difficult to address this phenomenon in a meaningful statistical way.

A basic question we would like to address is the question of how often the density minimum is observed. The equatorially trapped plasmas are a nearly ubiquitous characteristic of the equatorial region, at least at ambient plasma densities ranging from 10-100 cm^{-3}, occurring about 50% of the time [*Olsen et al* 1987, Plate 7]. The density minimum is less common - not every case of equatorially trapped plasmas showed a density minimum [e.g. *Olsen et al.,* 1987, Figure 16 and discussion thereof]. Indeed, one case has now been found where there is a small local maximum at the equator, in association with equatorially trapped ions.

Within the plasmasphere, the density minimum is associated with RIMS measurements of heated, but primarily isotropic plasma, as shown in the examples from 14 March 1983, and 15 March 1982. The local minimum deep within the plasmasphere, as seen on these two days, is relatively uncommon. Smooth distributions associated with diffusive equilibrium are the norm inside the plasmasphere (n > 200 cm^{-3}). In these latter two examples, both the cold H^+ and He^+ densities are reduced by at least a factor of 2. A hot tail forms at a density level which is ~1% of the cold density.

For the two cases within the plasmasphere with clear data (15 March 1982, Day 74; and 14 March 1983, day 73), we made the assumption that the heated plasma was ~isotropic in order to make the RPA analysis possible. If we continue with this assumption, we can consider the H^+ pressure balance across the density boundaries. Table 1 gives the cold, or core plasma parameters (indicated with a subscript "1") and the parameters for the hot tail (indicated with a subscript "2"), and the total H^+ pressure. For day 74, the pressure at the equator is substantially reduced, even when the warm component is included. For day 73, there is a rough balance. Indeed, the uncertainty in the cold H^+ measurement (caused by detector saturation), is enough to explain the difference.

If the anisotropy of the plasma is ignored, the illustration from day 52 shown by Olsen et al [1987], Plate 2], is similar to the one presented here for 8 January 1982 (Plate 3). On day 52, the density drops by a factor of 5 or so, but the pressure (nkT), remains approximately constant at 100 eV/cm^3 [*Olsen et al,* Figures 7 and 8]. A similar balance is found for the example from 16 March 1982 in the same article [*Olsen et al, F*igure 10].

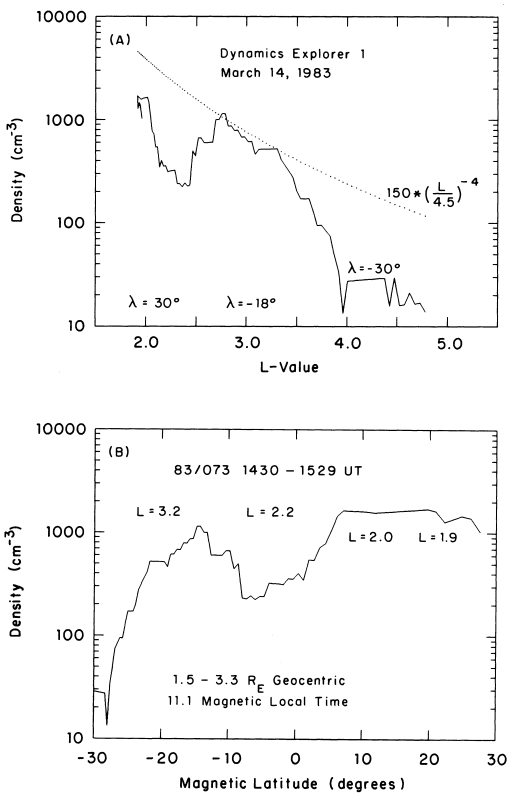

Figure 12. Density profiles for 14 March 1983 (Day 73). A) Total electron density versus L. An L-4 profile is superimposed. B) Electron density versus magnetic latitude.

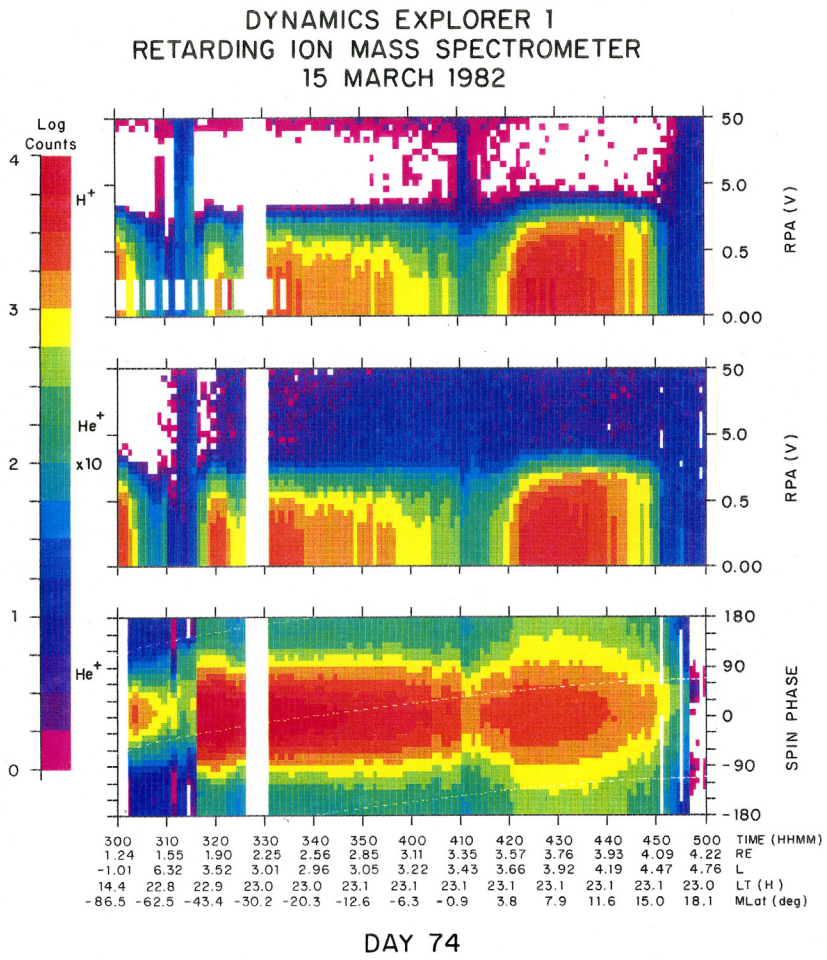

Plate 4. DE 1 data from 15 March 1982. The top panel shows H^+ RPA data from the end head. The middle panel shows the RPA analysis of the +Z detector measurements of He^+. The He^+ data have been scaled up by a factor of 10. Cold plasma is visible from 0315-0400, and 0415-0445. The bottom panel shows radial He^+ angular distributions for 0 V aperture bias. He ions with energies from 0-50 eV are measured. The angular distribution is that normally expected for isotropic plasma, e.g. ordered by spin phase, with the most intense fluxes in the ram direction (0° spin phase). The plasmapause at 0450 UT is marked by the end of the ram plasma distribution, and the beginning of field-aligned plasma measurements. The dotted white lines indicate the 0° and 180° pitch angle points.

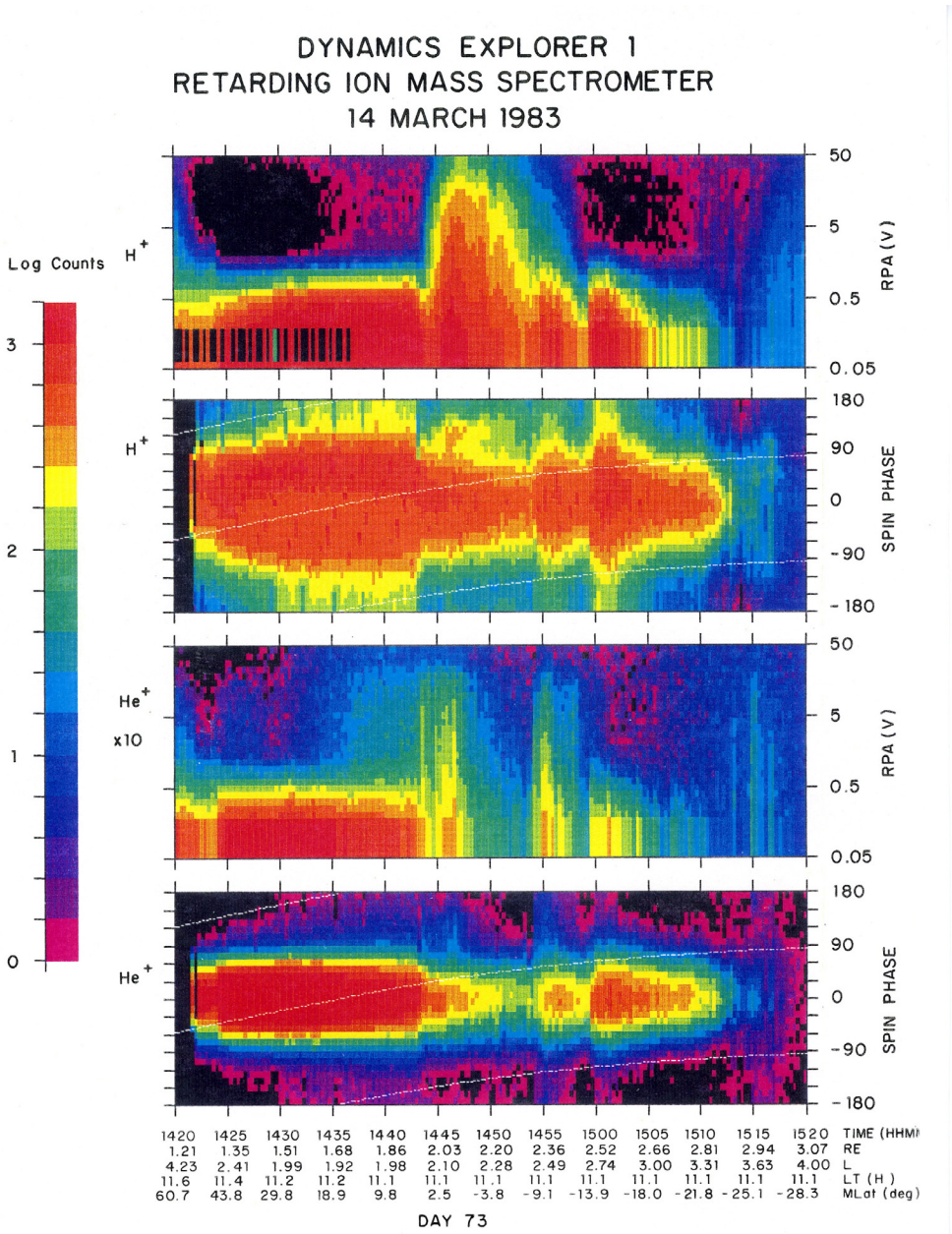

Plate 5. DE 1 data from 14 March 1983. H^+ and He^+ data from RIMS are shown. The top two panels show the H^+ data, the bottom two, He^+ data. The He^+ RPA data have been multiplied by 10 to bring the He^+ data onto the H^+ RPA scale.

In the plasmapause region (densities from 10-100 cm^{-3}), the density minimum is still typically associated with H^+ heating. A higher percentage of the thermal plasma is found at higher temperatures, particularly in H^+. The reduction in the cold plasma density, and a relative lack of He^+ heating, results in an apparent exclusion of the He^+ from the equatorial region. The measurements made in fall, 1983, in the dusk region are the ones which most typically reveal a density minimum. Here, the satellite is near apogee at the equator, and typically in the outer plasmasphere ($n < 100$ cm^{-3}). When the aperture bias is cycling, it is often possible to observe the depletion in He^+, as shown above for 23 October 1983. However, the smooth distributions characteristic of diffusive equilibrium, as shown by *Decreau et al* [1986], are still the most common latitudinal profiles in the dusk region. In the example for day 296 (Figure 5), there is an indication of a collisionless profile over the broader latitude range, which may indicate an early stage of refilling (Figure 7, *Decreau et al,* [1986]).

There are indications of a disconnection between hemispheres in some of the plasmasphere data. The density profiles in the two hemispheres vary in their L dependence. This characteristic of the data differs from the radial structure encountered with phenomena such as detached plasma regions, where, after the local minimum is encountered, the plasma density profile resumes its former trend [*Chappell,* 1974]

TABLE 1. Proton Pressure Balance

	Day 74 (0900 UT)	Day 73 (1500 UT)
	Off Equator	
n_1	500. cm^{-3}	1800. cm^{-3}
T_1	0.45 eV	0.40 eV
P_1	225. eV cm^{-3}	720. eV cm^{-3}
	At Equator	
n_1	175. cm^{-3}	300. cm^{-3}
T_1	0.55 eV	0.5 eV
P_1	96. eV cm^{-3}	150. eV cm^{-3}
n_2	0.35 cm^{-3}	15. cm^{-3}
T_2	35. eV	25. eV
P_2	12. eV cm^{-3}	375. eV cm^{-3}
P_{total}	108. eV cm^{-3}	525. eV cm^{-3}

3 DISCUSSION

The DE 1 orbits illustrated here present the idea of a local minimum in the plasma density near the magnetic equator. This minimum is not always observed. A general impression formed during this work is that perhaps 10-20% of the plasmapause passes show evidence for a minimum in density at the equator. This minimum is associated with heating of the thermal ions, which is much more commonly observed in this region. SCATHA data indicate electron heating also occurs in the outer plasmasphere [*Olsen,* 1981]. There is a rough balance in pressure for the H^+ across the density boundary.

This minimum in density can be interpreted as an important intermediate stage in the plasmasphere filling process. *Singh and Torr* [1990] have found a similar feature in numerical simulations of plasmasphere filling. Alternatively, the density minimum can be considered as a quasi-equilibrium state. This can be thought of as pressure balance, or as the result of an enhanced (positive) plasma potential. Heating of the low energy ions results in an increase of the plasma potential (of a volt or two). The ion density is then reduced by a factor exp (-qϕ/kT), and the electrons follow (basically a barometric law). This is the basis of the tandem mirror device, used for plasma confinement (fusion) experiments [*Dimov et al,* 1976*; Coensgen et al,* 1980]. Such effects will not be observed if the density is too high (the heating process is damped) or too low (the associated plasma temperatures are larger than the plasma potentials). The effect generally appears to be limited to a density range of 20-300 cm^{-3}, though the example from day 73 of 1983 occurs with a background plasma density of 1000 cm^{-3}.

It occasionally appears in the data that low energy, field-aligned ion beams are reflected, or bounced away from the equator. This interpretation has been suggested previously for DE 1 observations [*Olsen et al* 1987, Plate 5]. In the work shown here, the effect seems to be present in the data from 18 July 1982 [Plate 1]. *Singh and Hwang* [1987] find such an effect in their plasmasphere filling model. This again can be thought of as the result of an enhanced positive potential in the region near the equator. A reasonable consequence of such processes would be an effective disconnection between the hemispheres. This would be consistent with the variations in plasma density and character found in the data presented here, and previously.

Shock-like structures have been proposed as important intermediate states in plasmasphere filling [Banks and Holzer, 1968]. It is not clear how such structures should appear in thermal plasma data. The best resolved data are from the inner plasmasphere, in late stages of refilling. Data such as that from day 199, in a refilling region, are the most likely candidates. This example seems to show a collisionless background, with a density depletion (Figure 2.)

Further study of this phenomenon requires consideration of the plasma pressure effects, and pressure balance. In the cases which could be considered here, there was a rough pressure balance. Unfortunately, the parameter needed to determine this is the parallel temperature, which is not well measured by RIMS after the RPA failure. This becomes crucial when the plasma is anisotropic. The parallel temperature parameter may be obtained on a subsequent satellite. Also, for the many times when the density minimum is small the minimum tends to be difficult to measure. This is due to the spacing of the frequency steps of the plasma wave instrument. This is primarily a limitation imposed by telemetry, and would need to be addressed with an instrument dedicated to tracking the plasma density, such as the active experiments on GEOS 1 and 2.

Ideally, a pair of satellites such as ISEE 1 and DE 1 could be used to study this process. If so, the instruments need to be routinely operated such that data are always being collected, or substantial special efforts will need to be made to assure that complementary measurements are acquired.

4 ACKNOWLEDGEMENTS

My thanks to Don Gurnett and the late Stan Shawhan for allowing use of the DE/PWI data. C. R. Chappell was the DE/RIMS principal investigator, and provided many of the facilities used to analyze these data. The work presented here was supported by NASA/GSFC while the author was at the University of Alabama in Huntsville, under NAG5-568. Support was also received from NASA/MSFC under NASB-33982. Work done at the Naval Postgraduate School was supported by the Navy. W. K Peterson and E. G. Shelley provided the EICS data, and aid in interpreting the EICS data. EICS analysis at Lockheed Space Sciences Laboratory is supported under NASA contract NAS5-33032. Heavy use was made of the Space Physics Analysis Network (SPAN). Completion of this work was stimulated by the Huntsville Plasmasphere Refilling Workshop, in October 1990. Thanks go to Alan Biddle for pointing out the tandem mirror analogy, and references.

REFERENCES

Banks, P. M., and T. E. Holzer, The polar wind, J. Geophys. Res., 73, 6846-66854, 1968.

Brace, L. H., and R. F. Theis, The behavior of the plasmapause at mid-latitudes: ISIS 1 Langmuir probe measurements, J. Geophys. Res., 79, 1871-1884, 1974.

Carpenter, D. L., Whistler evidence of the dynamic behavior of the duskside bulge in the plasmasphere, J. Geophys. Res., 75, 3837-3847, 1970.

Carpenter, D. L., and R. L. Smith, Whistler evidence of a "knee" in the magnetospheric ionization density profile, J. Geophys. Res., 68, 1675-1682, 1963.

Chappell, C. R., Detached plasma regions in the magnetosphere, J. Geophys. Res., 79, 1861-1870, 1974.

Chappell, C. R., K. K. Harris, and G. W. Sharp, The morphology of the bulge region of the plasmasphere, J. Geophys. Res., 75, 3848-3861, 1970.

Chappell, C. R., S. A. Fields, C. R. Baugher, J. H. Hoffman, W. B. Hanson, W. W. Wright, H. D. Hammack, G. R. Carignan, and A. F. Nagy, The retarding ion mass spectrometer on Dynamics Explorer-A, Space Sci. Instrum., 5, 477-491, 1981.

Chen, A. J., and R. A. Wolf, Effects on the plasmasphere of a time-varying convection electric field, Planet. Space Sci., 20, 483-509, 1972.

Coensgen, F. H., et al., Electrostatic plasma-confinement experiments in a tandem mirror system, Phys. Rev. Lett., 44, 1132–1135, 1980.

Decreau, P. M. E., D. Carpenter, C. R. Chappell, R. H. Comfort, J. L. Green, D. A. Gurnett, R. C. Olsen, and J. H. Waite, Latitudinal plasma distribution in the dusk plasmaspheric bulge: Refilling phase and quasi-equilibrium state, J. Geophys. Res., 91, 6929-6943, 1986.

Dimov, G. L, V. V. Zakaidakov, and M. E. Kishinevskii, Thermo-nuclear confinement system with twin mirror systems, Sov. J. Plasma Phys., Engl. Transl., 2, 326-333, 1976.

Gallagher, D. L., P. D. Craven, and R. H. Comfort, An empirical model of the Earth's plasmasphere, Adv. Space Res., 8, 15–24, 1988.

Gringauz, K. I., V. G. Kurt, V. I. Moroz, and I. S. Shklovskii, Results of observations of charged particles observed out to R = 100,000 km, with the aid of charged-particle traps on Soviet space rockets, Astron. Zh., 37, 716-735, 1960.

Horwitz, J. L., R. H. Comfort, and C. R. Chappell, Thermal ion composition measurements of the formation of the new outer plasmasphere and double plasmapause during magnetic storm recovery, Geophys. Res. Lett., 11, 701–704, 1984.

Horwitz, J. L., L. H. Brace, R. H. Comfort, and C. R. Chappell, Dual-spacecraft measurements of plasmasphere-ionosphere coupling, J. Geophys. Res., 91, 11,203–11,216, 1986.

Kurth, W. S., J. D. Craven, L. A. Frank, and D. A. Gurnett, Intense electrostatic waves near the upper hybrid resonance frequency, J. Geophys. Res., 84, 4145-4164, 1979.

Olsen, R. C., Equatorially trapped plasma populations, J. Geophys. Res., 86, 11,235–11,245, 1981.

Olsen, R. C., C. R. Chappell, and J. L. Burch, Aperture plane potential control for thermal ion measurements, J. Geophys. Res., 91, 3117–3129, 1986.

Olsen, R. C., S. D. Shawhan, D. L. Gallagher, J. L. Green, and C. R. Chappell, Plasma observations at the earth's magnetic equator, J. Geophys. Res., 92, 2385–2407, 1987.

Shawhan, S. D., D. A. Gurnett, D. L. Odom, R. A. Helliwell, and C. G. Park, The plasma wave and quasi-static electric field experiment (PWI) for Dynamics Explorer-A, Space Sci. Instrum., 5, 535–550, 1981.

Shelley, E. G., D. A. Simpson, T. C. Sanders, E. Hertzberg, H. Balsiger, and A. Ghielmetti, The energetic ion composition spectrometer (EICS) for the Dynamics Explorer-A, Space Sci. In-strum., 5, 443-454, 1981.

Singh, N., and K. S. Hwang, Perpendicular ion heating effects on the refilling of the outer plasmasphere, J. Geophys. Res., 92, 13,513–13,521, 1987.

Singh, N., and D. G. Torr, Effects of ion temperature anisotropy on the interhemispheric plasma transport during plasmaspheric re-filling, Geophys. Res. Lett., 17, 925–928, 1990.

Taylor, H. A., H. C. Brinton, and C. R. Smith, Positive ion composition in the magnetoionosphere obtained from the OGO-A satellite, J. Geophys. Res., 70, 5769–5781, 1965.

R. C. Olsen, Physics Department, Naval Postgraduate School, Monterey, CA 93943.

(Received April 16, 1991; revised September 17, 1991; accepted October 28, 1991.)